

SPE 77646

## Lost Hills Field Trial - Incorporating New Technology for Reservoir Management

J. L. Brink, SPE, Chevron USA Production Company; T. W. Patzek, SPE, Lawrence Berkeley National Laboratory and University of California, Berkeley; D. B. Silin, SPE, Lawrence Berkeley National Laboratory; E. J. Fielding, Jet Propulsion Laboratory, California Institute of Technology

Copyright 2002, Society of Petroleum Engineers Inc.

This paper was prepared for presentation at the SPE Annual Technical Conference and Exhibition held in San Antonio, Texas, 29 September–2 October 2002.

This paper was selected for presentation by an SPE Program Committee following review of information contained in an abstract submitted by the author(s). Contents of the paper, as presented, have not been reviewed by the Society of Petroleum Engineers and are subject to correction by the author(s). The material, as presented, does not necessarily reflect any position of the Society of Petroleum Engineers, its officers, or members. Papers presented at SPE meetings are subject to publication review by Editorial Committees of the Society of Petroleum Engineers. Electronic reproduction, distribution, or storage of any part of this paper for commercial purposes without the written consent of the Society of Petroleum Engineers is prohibited. Permission to reproduce in print is restricted to an abstract of not more than 300 words; illustrations may not be copied. The abstract must contain conspicuous acknowledgment of where and by whom the paper was presented. Write Librarian, SPE, P.O. Box 833836, Richardson, TX 75083-3836, U.S.A., fax 01-972-952-9435.

### Abstract

This paper will discuss how Chevron U.S.A. Inc., a ChevronTexaco Company (ChevronTexaco), is implementing a field trial that will use research developed software integrated with Supervisory Control and Data Acquisition (SCADA) on injection wells, in conjunction with satellite images to measure ground elevation changes, to perform real-time reservoir management in the Lost Hills Field. Implementation of a new software control model to restrict hydrofracture growth in water injection wells is being field tested.<sup>1</sup> Synthetic Aperture Radar Interferograms (InSAR) are being obtained on an approximately 60-day interval to determine subsidence rates and will be used as an input variable for pattern voidage calculations. Incorporating new and innovative technologies is helping ChevronTexaco produce a very unique and challenging diatomite reservoir.

### Introduction

The Lost Hills Field was discovered in 1910 and is located approximately 45 miles northwest of Bakersfield, California (Figure 1). ChevronTexaco implemented a waterflood in the Lost Hills field in 1992 to increase recovery and mitigate subsidence.<sup>2</sup> Waterflood project oil production from the Belridge diatomite reservoir is approximately 10,000 BOPD and has been relatively flat for the last seven years (Figure 2). The majority of the 520 acre waterflood area is developed on 2½ acre staggered line drive patterns. Injection has been confined to the intervals from the F point to the K point (Figure 3).

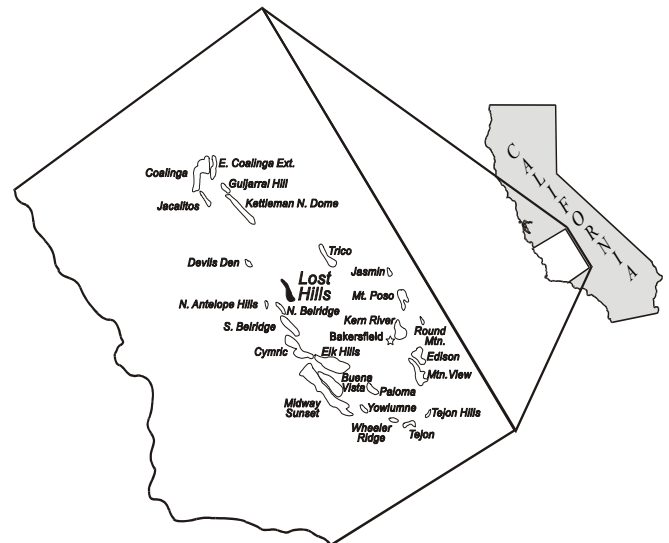


Figure 1. Lost Hills Field location map.

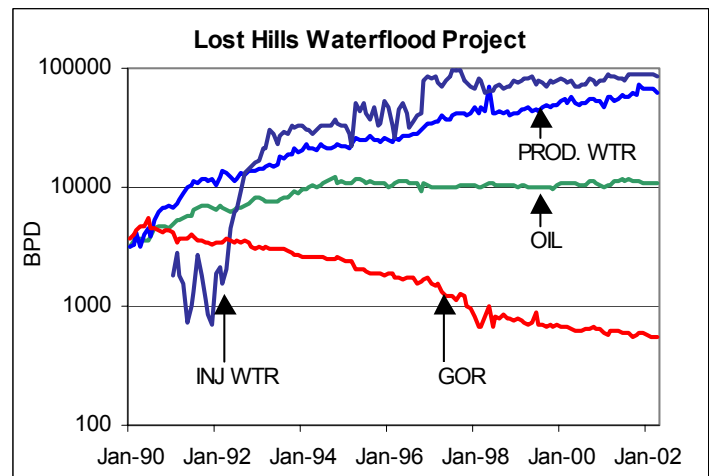


Figure 2. Lost Hills Waterflood Project - production and injection plot.

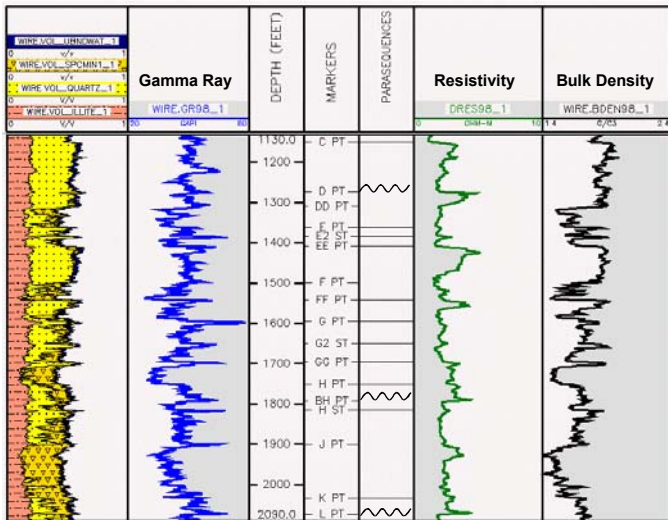


Figure 3. Type log for typical Lost Hills waterflood well.

In 1999, nine 1¼ acre line drive patterns were piloted to test the feasibility of reducing the pattern size to increase oil recovery. Successful results from this pilot have led ChevronTexaco to proceed with implementing 30 additional 1¼ acre patterns in 2002. Sixteen 5/8 acre staggered line drive patterns were completed in 2001 to investigate the ability to recover additional reserves by reducing the pattern size even further.

Managing a waterflood with injection and production wells only 100 feet apart is very challenging, now add the complexity of subsidence. Controlling water break through with wells only 100 feet apart seems almost simple when you have to deal with the ground sinking too.<sup>3</sup> Portions of the field have subsided over 10 feet since 1989 creating numerous mechanical wellbore failures. Several new and innovative techniques have been implemented to remediate casing damage, including the use of expandable casing systems.<sup>4</sup> To successfully waterflood this tightly spaced, low permeability diatomite rock, a detailed and comprehensive reservoir management plan must be in place to monitor the performance. Reaction time to well communication must be almost instant to minimize the long-term negative effects it can have on oil recovery. Implementing the injection control model and utilizing InSAR to measure subsidence will likely enable ChevronTexaco to extend the life of the Lost Hills field.

### Current Monitoring Program

The waterflood project is located on Sections 4, 5, 32 and 33 and has 327 producers and 228 injectors (Figure 4). An extensive surveillance program has been in place since the project began to capture data pertaining to well tests, reservoir pressure, vertical and areal sweep efficiency, and fracture direction. These data are critical to assess the effectiveness and efficiency of the waterflood. Subsidence related data have also been captured to monitor and predict well failures due to mechanical damage. Data that have been captured is then

stored in ChevronTexaco's Reservoir Management Information System (RMIS) database. This database serves as one of the integral pieces of the Lost Hills reservoir management plan.

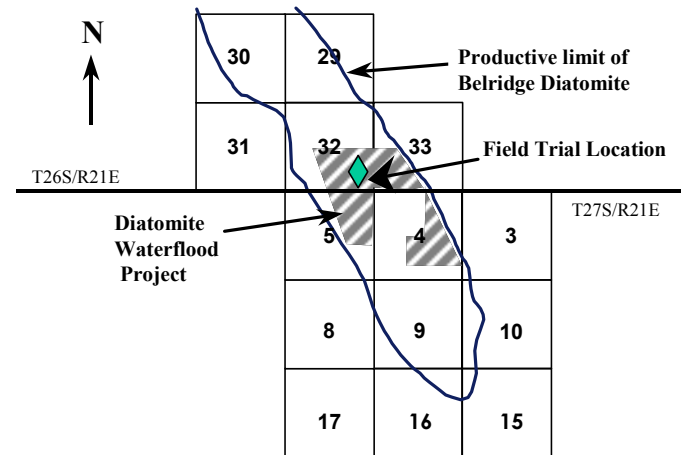


Figure 4. Waterflood project area and field trial location.

**Well Tests.** Determining and measuring fluid volumes are critical to understanding the success or failure of any reservoir related field trial. ChevronTexaco is substantially invested in obtaining accurate and reliable well tests in the Lost Hills field.

**Production Wells.** The 327 rod-pumped production wells in the project area are all equipped with pump off controllers (POC). All producers are connected to intermediate collection stations known as gauge settings where the well tests are performed before the oil is cleaned and shipped for sales. The gauge settings are fully automated to test wells in a predetermined order. Well tests are taken on average every six days. Oil, water and gas rates are obtained and transmitted to a central database in the office via the network. Fluid cuts are determined using a Coriolis Mass Flow Meter. Oil and water densities are measured at the laboratory for calibrating the Coriolis Meter. These data are then stored in ChevronTexaco's Geochem database for future use.

**Injection Wells.** There are 228 injection wells of which 114 are dual completion and 114 are single completion. Dual completions were common in the early development of the project as a method to try to mechanically achieve better vertical conformance. Since 1998, only single completions have been drilled to minimize subsidence related mechanical problems. Injection well volumes are measured using a turbine meter. Injection well tests are gathered every two weeks. An instantaneous rate is read from the turbine meter. The volume is also determined from the difference between the last two meter readings. Both of these figures are entered into a handheld device terminal (HHDT) which is then uploaded to the central database base via docking the HHDT to the network.

**Reservoir Pressure Data.** Collecting and interpreting reservoir pressure is very important in understanding the functionality of a waterflood. Injection step rate tests have been performed over the life of the project to determine the parting pressure of the formation. Injecting below parting pressure is crucial to minimize the possibility of creating channels to the production wells. The parting pressure has increased over the life of the project as reservoir pressure has risen due to the waterflood. Injecting just below the parting pressure will insure the maximum amount of water will be injected without increasing the possibility of channeling. This will also help distribute the maximum amount of pore pressure support to keep the diatomite from collapsing. Injecting above the parting pressure, especially in the soft diatomite, will focus support on only a limited channel, thus increasing the possibility of the rock matrix collapsing.

**Sweep Efficiency Data.** Evaluating the sweep efficiency is critical to determining the overall success of a waterflood. Understanding the current sweep efficiencies prior to the field trial were important to determine if an improvement occurred after applying the technologies.

**Vertical Sweep Data.** Injection profile surveys are run every two years to determine the vertical sweep efficiency. The profiles are reviewed immediately to make sure no significant channeling develops. The data are stored in the RMIS database and can be re-displayed using standard surveillance software. A study was performed in 2001 to review the historical profile data. The study indicated that regardless of a dual or single completion type, hydraulically fractured or not, the injection was only entering into approximately 45% of the perforated intervals (Figure 5).

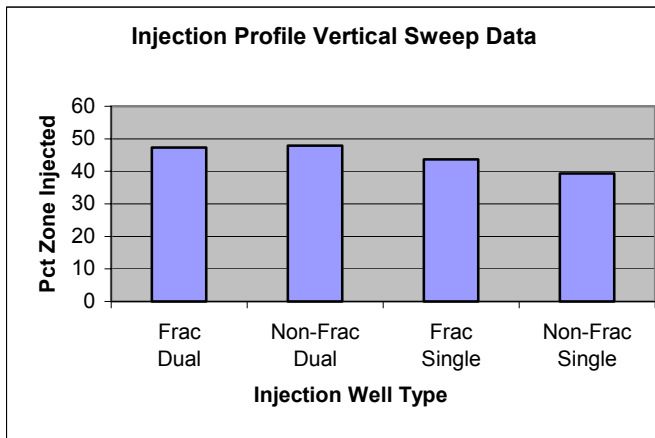


Figure 5. Injection profile data for all waterflood project injectors.

Based on the numerical simulations<sup>5</sup>, about half of the injected water may imbibe into the formation and the other half may flow through the high permeability flow paths linking an injector with the producers.

There is an annual remedial program in place to stimulate the injection wells that are not able to achieve the necessary replacement volumes to maintain reservoir pressure.

Stimulation is also used to increase the vertical distribution of the injected water.

**Areal Sweep Data.** Several areal sweep studies have been conducted in the past to determine flow paths between injection and production wells. These tests have included chemical tracer, crosswell electromagnetic (EM) imaging, and tiltmeter. There have been many very interesting and unusual results from these studies.

**Chemical Tracer.** A chemical tracer test was performed in Section 32 on well 9-8WA. The injection well has a dual string completion and different chemical tracers were injected into each of the strings. A tracer injected into the short string showed up in an offset production well in as little as 65 hours. The second author analyzed this test and concluded that the tracer flowed along essentially one-dimensional “tubes”. The link-tube permeability was estimated from the tracer breakthrough times for each of the production wells. The calculated permeability and pore velocities for four offset producing wells are shown in Table 1.

Well name	Tube length (ft)	Pore velocity (ft/d)	Permeability (md)
9-8A	140	53	180
9-8QA	230	10	57
10-8A	230	10	56
175A	280	8	53

With the currently assumed water production rates of 100 bbl/day for each of these four production wells, the flow tube cross section can be estimated to be from 1x30 cm to 1x180 cm in size. Figure 6 shows that the calculated link-tube permeability agrees well with the air permeabilities (of core damaged or naturally fractured core plugs) from observation well OB-7, located in Section 32. The reservoir rock around OB-7 was not disturbed considerably by water injection.

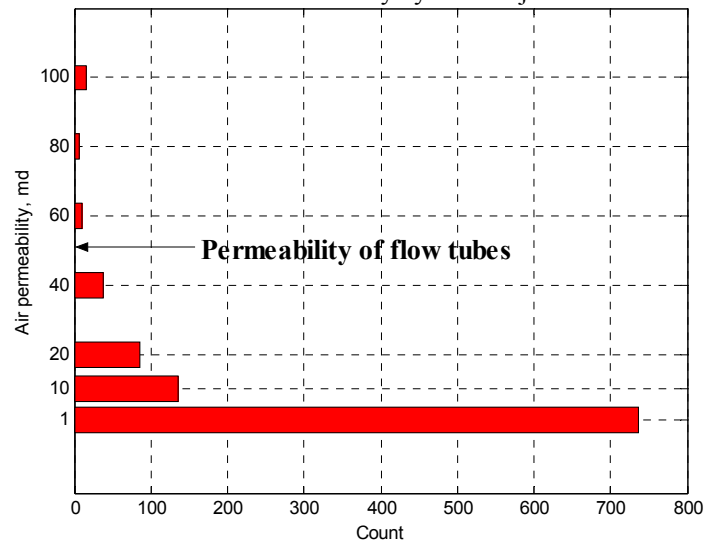


Figure 6. Frequency distribution of air permeabilities of core plugs from well OB-7. Note that most core plugs have permeabilities between 0 and 1 md.

*Electromagnetic Data.* Crosswell EM has been performed in the Lost Hills field using two separate systems<sup>6</sup>. The first system was deployed in fiberglass-cased wellbores which straddled water injection well 10-9W. The crosswell EM was run to try and identify vertical sweep (resistivity changes which would indicated flood fronts), interwell structure and any associated barriers to flow. Figure 7 shows the resistivity cross section between the two fiberglass-cased wellbores (OB-7 and OB-8). The cross section shows that even over a distance of 100 feet, the resistivity distribution observed in the logs is not the same over the pattern area.

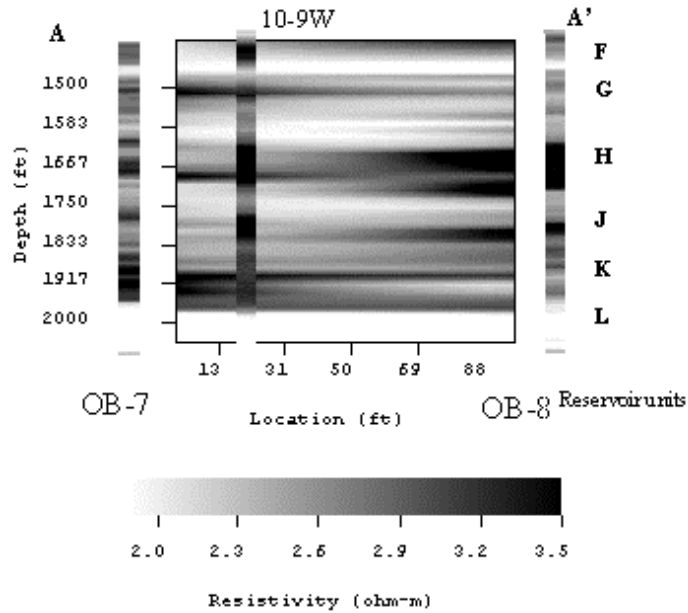


Figure 7. EM cross section showing resistivity change.

*Tiltmeter Data.* Surface and downhole tiltmeter data have been collected in the past to determine fracture orientation and fracture height<sup>7-9</sup>. Most of this data have been collected during hydraulic fracture treatments. There have been approximately 500 hydraulic fractures mapped since 1987, indicating an average fracture azimuth of N47°E ±10°.

**Subsidence.** A comprehensive monitoring program to measure subsidence has been in place since the initiation of the waterflood project. Every six months, permanently installed survey monuments are measured using Global Positioning Satellite (GPS) measurements to determine ground surface movement. Currently there are 142 monuments. Additional monuments have been added over the years in the pilot areas to monitor subsidence more closely. A map showing cumulative subsidence from 1989 to 2001 is shown in Figure 8. Lateral movement of the survey monuments is also monitored. Movement of the monuments is toward the center of the subsidence bowl, as seen in Figure 9. The vertical subsidence puts the casing in compression and the lateral movement adds a shear component. Casing failures have consisted of doglegs (shearing or parting) and buckling.

In addition to surface measurements, radioactive markers have been placed in selected wells to determine downhole compaction. The radioactive markers, 50 microcurie Cobalt wires, were placed in the wells with a sidewall core gun. Gamma ray logs are being run in the wells annually to determine vertical movement.

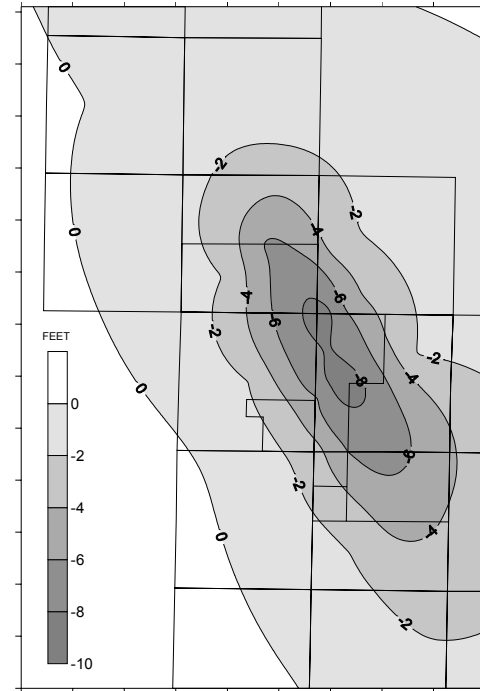


Figure 8. Cumulative subsidence from 1989-2001 using GPS measurements.

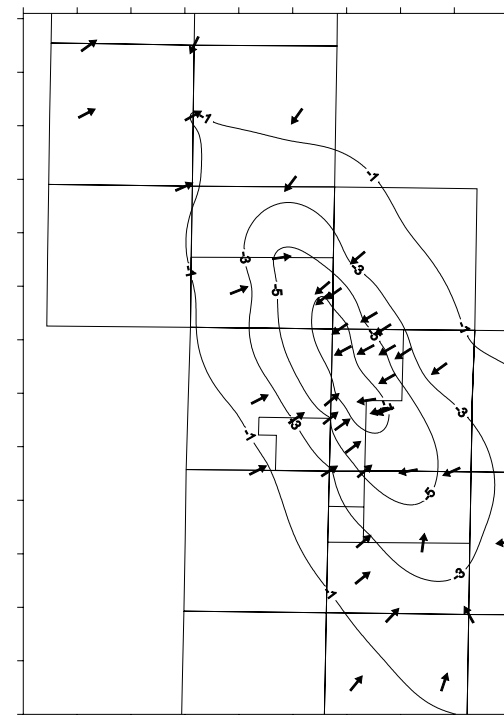


Figure 9. Vectors showing lateral movement.

## Control Model Development and Design

The purpose of control is stabilization of injection at a given rate by adjusting injection pressure. The distinguishing property of the proposed control scheme is that it is model-based. We use the model of injection into a layered reservoir developed in papers<sup>1, 10, 11</sup>. In this section, we overview the model and describe the control procedure implemented in the Lost Hills field trial.

**Injection model.** The model on which we base our control system was first developed for injection into a single fractured well in a homogeneous reservoir<sup>10, 11</sup>. Later, it was extended to injection in a layered reservoir<sup>1</sup>. The diatomite formation has a layered structure with varying thickness for each of the different lithological units. The layered heterogeneity resulting from the depositional environment leads to development of high-permeability channels connecting injecting and producing wells. Therefore, the total flow from the well into the formation is the sum of transient and steady-state flow components. The transient flow at a constant pressure is characterized by the square-root-of-time scaling of cumulative injection, whereas the steady-state flow follows a linear time scaling. At mature transient flow (where the slope of injection versus time curve changes very slowly), the time scale needed to distinguish between the transient and steady-state modes is large.

The conclusions we derived from the model and field data suggest that the current injection rate at an individual well is determined not only by the instantaneous injection pressure, but by the whole history of all previous operations. This rate depends on the formation properties: permeability and hydraulic diffusivity, on the injection pressure and on the size of the hydrofracture. To characterize the last parameter, we introduced an “effective” fracture area. An important feature of the model is that the fracture size is not a constant but it may change in the course of operations. We call this parameter “effective” for several reasons. First, the actual geometric dimensions of the fracture are unavailable for measurement. Second, the fracture itself is not a perfect geometric structure but a region of the formation with extensive rock damage<sup>12</sup>. Finally, the fracture may consist of numerous defects at different scales, which are connected to the wellbore and may coalesce into macroscopic structures. The parameter we introduced has the dimensionality of area, therefore we use the term “effective” area.

Following the square-root of time scaling, the transient flow is dominant at early times of waterflood. If the formation properties remain constant, then with time the transient flow become mature and the steady-state component becomes dominant. To characterize the distribution of the injected fluid between the transient and steady-state flow, two lumped parameters were introduced. These parameters depend on the effective fracture area, formation permeability and hydraulic diffusivity, relative permeability with respect to water, and water viscosity. For consistency with paper<sup>1</sup>, we denote these parameters by  $Y$  and  $Z$ . The squared ratio of  $Y$  and  $Z$  has the dimension of time. It characterizes the length of the time

interval over which the steady-state mode of the flow becomes dominant over the transient flow component.

We further assume that the fracture extension and rock damage propagation are not continuous processes like fluid flow, but they happen in relatively short increments at discrete moments of time. Therefore, the two parameters introduced above are piecewise-constant functions of time.

The model has been verified against field data. The results of verification are presented on Figure 10 and Figure 11. The circles on Figure 10 are the cumulative injection data calculated based on the injection rates measured on daily basis. The solid line is calculated using the model<sup>1</sup>. Five points on the 450-days observation interval were selected as possible moments of formation properties changes caused by possible fracture extension or collapse caused by subsidence. The plot on Figure 11 shows the estimated parameter characterizing the transient portion of the flow as a function of time. The calculation of this parameter involves injection pressures. The jagged line shows the results of calculations based on daily measured pressures, whereas the piecewise-constant line plots the same parameter calculated using injection pressures averaged over the respective time intervals.

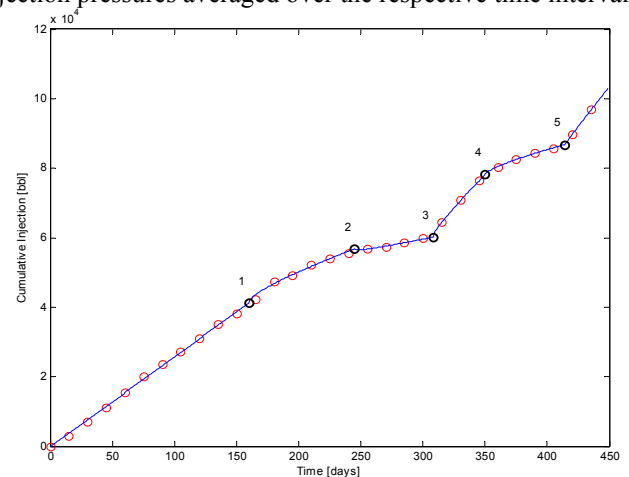


Figure 10. Cumulative injection plot: solid line depicts calculated injection, the circles plot the data points.

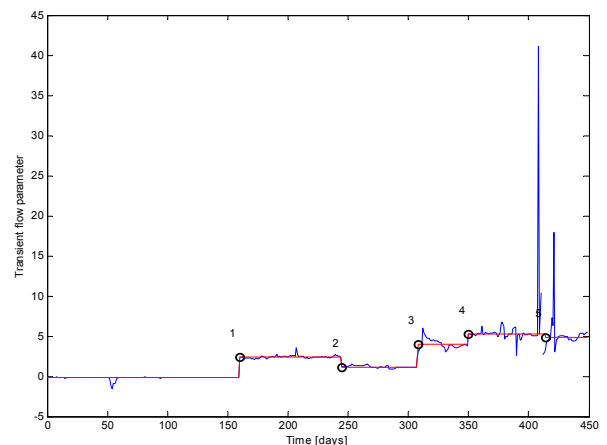


Figure 11. Transient flow parameter. The piecewise constant line is based on pressures averaged over respective intervals.

One can see that at the beginning, the well operates in mostly steady-state mode. Then, at point 1, a possible fracture extension causes increase of the transient flow parameter. This parameter then experiences further variations. It is interesting to note that although the transient mode of the flow is increasing in time, it is substantially dominant only between points 4 and 5. This conclusion cannot be derived exclusively from the plots in Figure 10 and Figure 11, but follows from the estimation of the characteristic time parameter mentioned above. The analysis above was performed using standard parameter estimation and optimization techniques. The points of possible breakthrough or other formation perturbations near the well were selected by visual inspection of data. The data were obtained over an extended time. The time intervals between the numbered points in plots in Figure 10 and Figure 11 are in the order of months.

**Control Design.** According to our model, to design a day-by-day injection control providing stable injection rate, we need to have a capability to have at our disposition means to measure or estimate the parameters characterizing the transient and steady-state mode of the flow at sufficiently frequent times. To obtain such estimates, we have developed a procedure, which analyzes the injection pressure-cumulative injection data in order to estimate the current flow distribution. As we have already mentioned above, the current instantaneous flow rate is not a function of only current injection pressure and current flow distribution parameters. It is a function of the history of operations as well. Therefore, the control cannot be designed as a genuine closed-loop feedback system. The injection pressure and rate measurements, along with the estimates of the flow parameters obtained at earlier times, have to be retained for future calculations. The injection pressure set point for the next planning interval is then determined by analyzing all these data.

The control model schematic is presented in Figure 12. The database stores historical injection pressures ( $P$ ), injection rates ( $Q$ ), steady state ( $Y$ ) and transient flow ( $Z$ ) parameters. These values are then linked to the control and fracture diagnostics modules. The fracture diagnostics module analyzes the current measurements along with the historic data and estimates the current values of  $Y$  and  $Z$ . These parameters are then input into the control module, which computes the pressure set point. Besides the parameters  $Y$  and  $Z$ , the control module also analyzes the historical data and the output is computed based on injection rate set point. As it has been mentioned above, the control cannot be designed as a genuine feedback regulator because an injection well is a system with memory. Therefore, the control is planned over a certain planning interval. The pressure set point is determined constant for each individual interval but can be different from one interval to another. At the beginning of a control planning time interval, the current values of parameters  $Y$  and  $Z$  have to be available. The injection pressure set point is obtained by minimization of a quadratic criterion, which evaluates on the planning interval the deviation of the cumulative injection

computed according to our model from the target cumulative injection. The target cumulative injection is easily calculated by integrating the target injection rate. By the end of a control planning interval, a new one has to be generated and this procedure is iterated in time. At the start of the control, some time is needed so that the control parameters, such as reservoir pressure or pumping pressure, can be calibrated. At later time, the contribution from the early history data becomes negligible. Therefore, the history database needed for computations can be truncated and its volume will not indefinitely grow during years of operations.

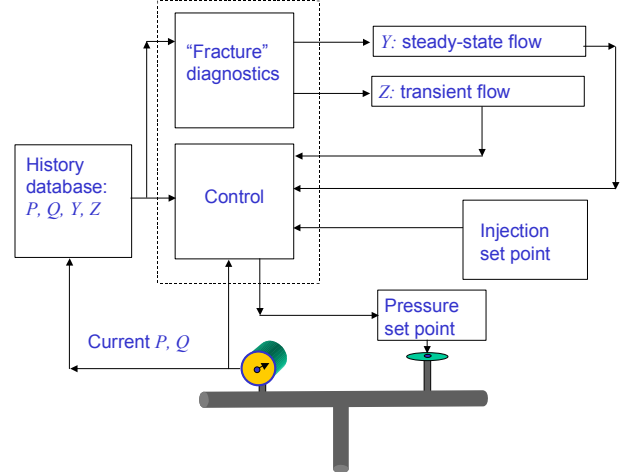


Figure 12. Control model schematic.

Selection of the length of control planning interval is limited by several factors. On one hand, the example presented in Figure 10 and Figure 11 demonstrates that the characteristic time where the transient flow component can be separated from the steady state component is measured in months. On the other hand, such a time scale is practically unacceptable because the control system has to be able to promptly react to changing injection conditions. It turned out that control planning time interval of one day (24 hours) is a reasonable compromise. Also, one day is the usual operations life cycle.

To test the procedure described above, a 43-days data interval was selected. To imitate real time control, these data were passed to the controller in chunks, day by day. The fracture diagnostic module analyzed these data and saved the estimated values of  $Y$  and  $Z$  along with the end times of the planning intervals. The control module loaded these data and computed the output injection pressure set point for the next planning interval. The first four days of the data were selected as the initial calibration time interval.

The injection pressures and injection rates data were collected every minute. Pressure transducers measure the injection pressure with a remarkable accuracy. At the same time, the flow rates measurements are accompanied by noise. This was one of the motivations of developing the control procedure as described above. Indeed, our computations deal only with cumulative injection, therefore the noise in the

injection rates data, Figure 13 is smoothed out in cumulative injection by integration, Figure 14.

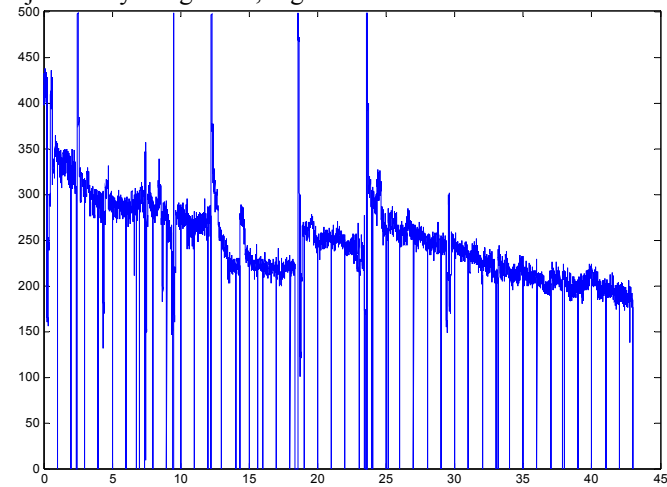


Figure 13. Injection rates in bbl/day versus time in days.

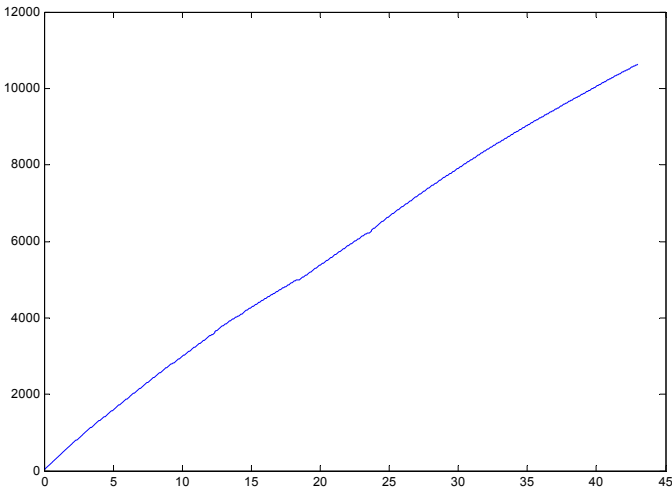


Figure 14. Cumulative injection in bbl/ versus time in days.

To imitate real time control, the target injection rate for the next planning interval was computed based on actual injection on this interval. In other words, the cumulative injection over the next planning interval was divided by the interval length. The computed set point pressures were compared with the actual pressures. The results are presented in Figure 15. The jagged line is the plot of actual pressures, whereas the bold solid line consisting of straight intervals is the plot of computed pressure set points.

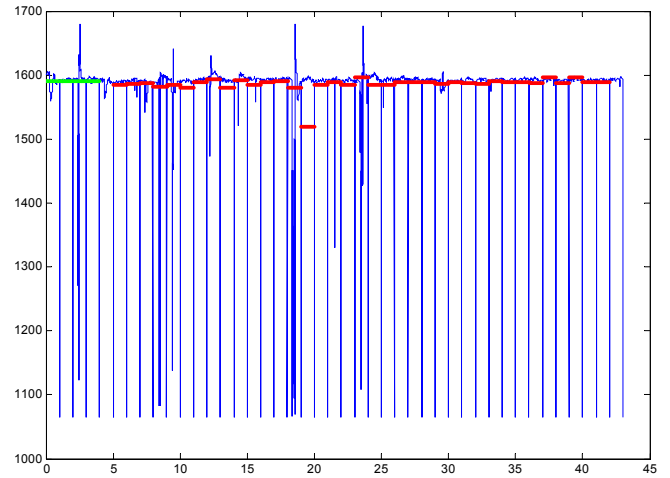


Figure 15. Injection pressures in psi versus time in days.

As it has been mentioned above, the one-day planning period is a reasonable compromise between the characteristic time scale needed for separating square-root of time transient flow mode from the steady-state flow. Therefore, an overall look back from time to time may be needed for a better understanding of character of the flow. This can be clearly seen on the estimates of the flow parameters  $Y$  and  $Z$  obtained by the fracture diagnostics module. The plots are presented in Figure 16 and Figure 17. The changed flow conditions on day 19 caused a “transfer” of some value from transient mode  $Z$  to steady-state mode  $Y$ . The overestimated value of parameter  $Y$  resulted in insufficient pressure set point, Figure 15. Later the magnitude of the initial spike decreased in square-root of time mode (dashed line). Therefore, the sharp increase in the steady-state mode parameter does not necessarily mean a water breakthrough but could be a result of misinterpretation resulted from the contradiction between the intrinsic time scale of the process and the practical necessity to implement control based on a shorter time period. In any case, a substantial presence of steady-state mode flow is noticeable. This observation confirms the sweep efficiency analysis presented above.

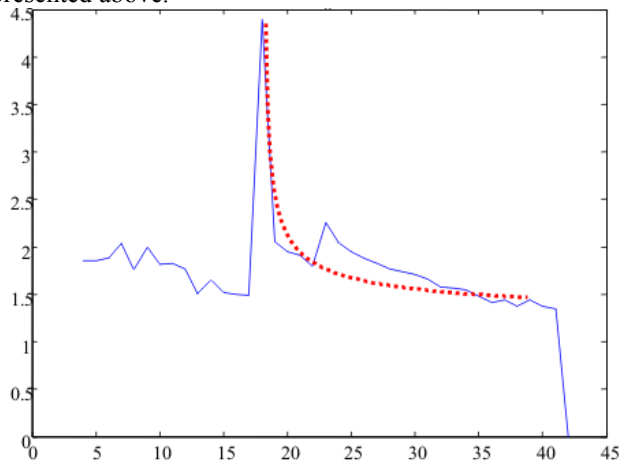


Figure 16. Steady-state flow parameter  $Y$  versus time in days. The dashed line corresponds to square-root of time scaling.

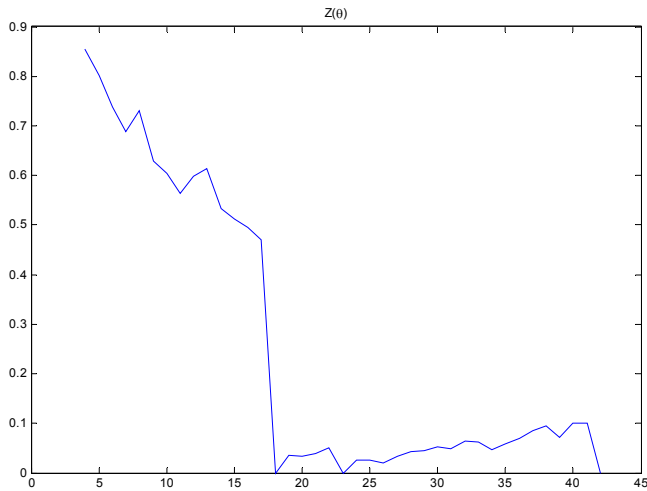


Figure 17. Transient flow parameter  $Z$  versus time in days.

### InSAR Data

Synthetic Aperture Radar Interferograms (InSAR) of the field surface are used routinely in California<sup>3</sup>. In the last few years, InSAR has become a very attractive technique to obtain more information from SAR images, see references<sup>13-15</sup> and references therein. Both the amplitude of the signal and its phase are used. Usually, two SAR images of the same region are acquired with slightly different sensor positions, and combined together. SAR Interferometry can be performed either using data collected by repeat-pass or single-pass sensors. The former implies the same antenna is used twice while the latter requires two distinct antennas to be flown aboard an aircraft or satellite.

InSAR and GPS datasets are acquired at different scales. A GPS station reading yields a highly accurate and precise measurement of ground motion *at a point*. Then 142 such measurements are interpolated (kriged) over an area of some 13 square miles. By its very nature the kriging process smoothes the subsidence contours significantly. The InSAR image consists of pixels, about 20-by-20 m in size, and the local line-of-sight ground motion is averaged over each pixel. Each individual pixel measurement is less precise than GPS, however, there are hundreds of *thousands* or millions of pixels in a single InSAR image and they cover the entire field area. No kriging is necessary to render a global picture of subsidence. Therefore InSAR images can pick up those features of subsidence that are impossible to capture with 142 GPS data points, and they complement the GPS surveys.

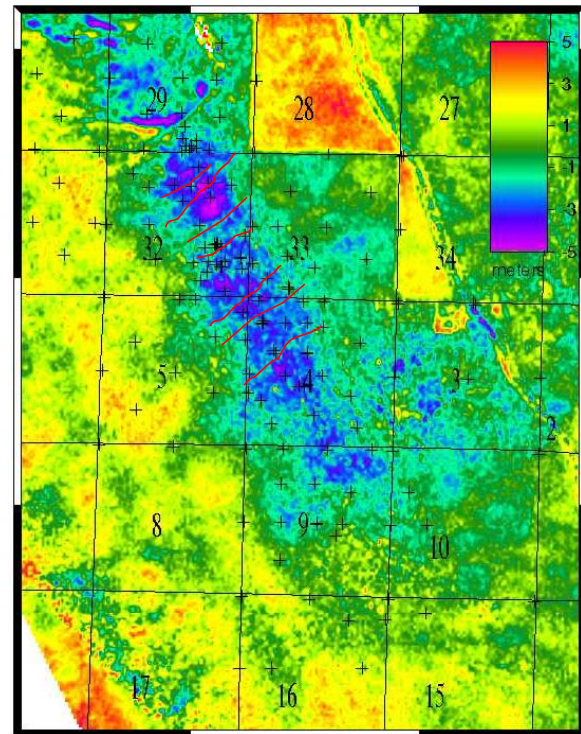


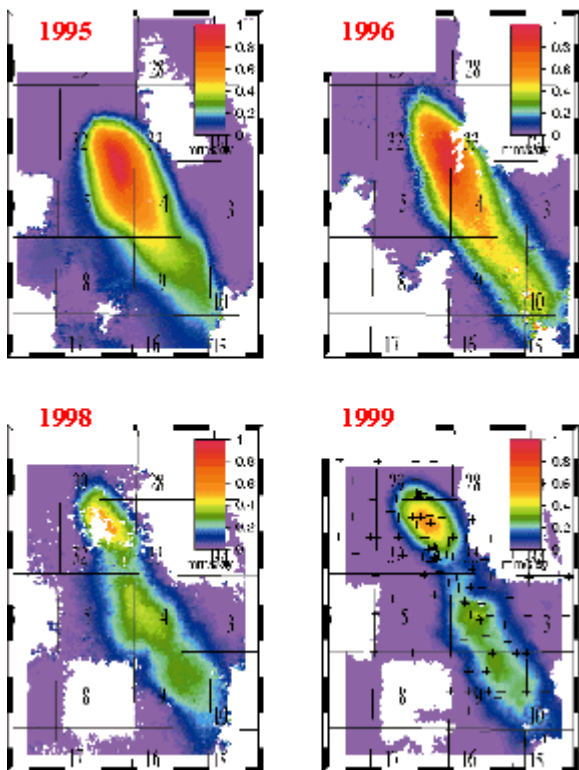
Figure 18. The difference of two Digital Elevation Model images of Lost Hills showing the cumulative effect of 17 years of vertical surface displacement in meters. The red and yellow areas in Section 28 and 34 are the orchard trees that grew to a height of 2-5 meters. The blue and purple areas outline the Lost Hills oilfield, where there was about 3 meters of subsidence. The red lines are the surface traces of the faults along the crest of the Lost Hills anticline. The crosses locate the GPS obelisks used to triangulate the land surface.

Figure 18 shows the difference between two different digital elevation models separated in time by 17 years. The first image was acquired by the USGS in 1982, and belongs to the National Elevation Dataset, NED<sup>16</sup>. The second image was acquired by the NASA/JPL TopSAR airborne system (which uses repeat-pass SAR interferometry) in 1998-1999. The USGS NED (<http://gisdata.usgs.gov/ned/>) has a grid spacing of 1-arcsecond or about 30 m. The TopSAR elevation data have a grid spacing of 10 m, but there is noise in the image, so it is not usually possible to resolve features as small as 10 m. The difference image has the 30-m resolution of the USGS NED. Because the image is the difference between two elevation datasets, it shows purely vertical displacement. Note that there is an additional source of error in the measurements because the TopSAR radar system is reflecting off of tree branches and oil pumps, etc., that are above the ground surface, while the USGS NED is the “bare earth” ground surface. Thus in Sections 28 and 34 the orchard trees that grew<sup>1</sup> to a height of 3-5 m are clearly visible. The reflections off of the oil extraction equipment may also contribute to the apparent bumpy nature of the difference in the oil field. The

<sup>1</sup> Confirmed by the visual inspection of the Lost Hills area in March 2002.



blue-purple outline of the producing field area subsided by about 3 meters. Figure 18 appears to show variations in elevation changes (unfortunately close to the noise level of the TopSAR data) that correlate with the normal faults identified by the ChevronTexaco geologists. Because these faults divide subsidence into compartments, they should also divide the flow of fluids in the diatomite into the similar compartments. Figure 18 may be the first direct evidence of the possibly major role of faults in determining the fluid flow field in the Lost Hills diatomite. This intriguing insight gained from the InSAR images needs further verification by the geologists and reservoir engineers.



**Figure 19.** The line-of-sight rate of subsidence at Lost Hills in mm/day. The differential ERS-2 satellite images have been processed by E. Fielding. The rate of subsidence at Lost Hills has decreased significantly between 1995 and 1999, mostly because of water injection.

Figure 19 shows the differential satellite InSAR images of Lost Hills. The line-of-sight rate of displacement of surface in mm/day is color-coded from purple (0 mm/d) to red (1 mm/d). The white areas are the image pixels that are de-correlated due to noise or excessive subsidence. Each of the four images in Figure 19 is a difference of two interferograms acquired by ERS-2. The InSAR images demonstrate that the rate of subsidence diminished significantly between 1995 and 1999. As shown elsewhere<sup>3</sup>, the satellite images can be used to calculate the cumulative volume of subsidence, and elucidate the major oil production mechanisms. Analysis of the InSAR images and field production/injection data leads to the conclusion that:

1. the injected water provides pressure support

2. much of the injected water is recirculated, while some imbibes into the formation
3. compaction drive is a significant component of hydrocarbon production.

Recently a new model of damage propagation in the soft diatomite was proposed<sup>17</sup> to quantify the field observation.

### Field Trial Implementation

Implementing the field trial has progressed through many stages through 2001 and 2002. InSAR data has been gathered for the years 1999 to 2001 and work has been done to calibrate it with the existing GPS data. Fabrication of the automated injection header took place in the 1st quarter of 2002. Ten injection wells were included in the pilot.

Modifications to the SCADA software were made to accommodate the water injection variables and accept input of these data from the controller model.

**Objectives and Design Considerations.** The main objectives of the field trial were to test the feasibility of implementing a laboratory developed theoretical control model to restrict hydrofracture growth and measure subsidence on a much finer scale using satellite technology. Secondary objectives, concerning the automated injection header, were to test the hardware components of the injection header, which brand of valves, flow meter and pressure gauge to use. Figure 20 is a photo of a portion of the automated injection header.



**Figure 20.** Automated injection header

In order to analyze the effects of the field trial, the pilot needed to be located in a portion of the reservoir that did not have any other tests or pilots in progress. This was very challenging with an aggressive drilling program in place for 2002 and several other field trials ongoing. The final field trial location was then selected where the least amount of activity was going to take place in the next 12 months.

Additional consideration was given to test the range of reservoir conditions, such as reservoir pressure, vertical and areal sweep and productivity of the wells.

**Operation and Surveillance.** Each of the wells in the field trial area were reviewed and baseline data was established. The baseline data for the injection wells included establishing historical trends for water injection rate and pressure, injection profile and Hall plot. The production wells baseline data include historical trends for oil, water and gas volumes, fluid level and pump cycle times. Production and injection volumes were also analyzed on a pattern basis. Oil production rate forecasts were made for each of the patterns in the field trial area.

The InSAR data is processed and received approximately every 60 days. ChevronTexaco receives the data by two methods. The first method is in the form of a digital picture similar to the ones in Figure 19. This method is good for visual analysis and using for presentations. The second method is in the form of a computer file. The file contains a row of data for each waterflood pattern identified by ChevronTexaco. Each pattern then has an associated value (in barrels) for the amount of subsidence, or dilation, for that pattern. These values are then included in the pattern balancing analysis performed for the waterflood each month.

Since the automated header has been in place only a short time as of the writing of this paper, no definitive conclusions have been drawn by switching from the manually controlled injection rate method to the new software based control model method. There has not been sufficient time to evaluate the long term effect on production and injection rates, or change in vertical or areal sweep efficiencies. ChevronTexaco is currently in the process of evaluating these data on an ongoing basis.

We have seen some very interesting interactions between some of the production and injection wells. One injection well experienced some very stable, but cyclic injection rates. It was noticed that it would be injecting at 250 bbl/day and then all of the sudden it would be injecting at 350 bbl/day for a period of time, and then return back to 250 bbl/day. The time intervals were almost cyclic in nature. One explanation that is being investigated is that one of the offset production wells was cycling on and off at the same intervals as noted with the increased injection. This could indicate that when the production well cycles on and begins to pump, a sudden pressure drop linkage to the injection well is taking place, thus allowing more water to be injected.

Understanding and being able to react almost instantaneously to these types of problems will allow ChevronTexaco to perform almost real time reservoir management.

### Future Plans

While the field trial has only been in place a very short time, the initial results have been very encouraging. Implementing new technology that enables ChevronTexaco to proactively manage this complex diatomite reservoir is attractive.

ChevronTexaco has placed money in future year budgets to automate the existing injection headers.

Additional plans for the future include incorporating production data into the control model. Incorporating information about the known, or perceived connections, between the injection and production wells, will allow an additional parameter to be considered for pattern balancing. For example, if Producer A experiences a sudden increase in water production, the fluid level would begin to rise and it might not be able to obtain a pump-off condition. This condition would set off a flag in the control model which would then seek out the injection well (call in Injection Well A) that most likely broke through. The control model would then use a set of business rules, or trained response, to systematically throttle back that injector until Producer A began to return to a pumped-off state. If this did not happen, the control model would restore Injection Well A to it's original rate and begin the same procedure on Injection Well B.

### Conclusions

The following picture emerges from the analysis of the production/injection rates, core, tracer and satellite data:

1. The undamaged Lost Hills diatomite is almost impermeable, Figure 6. Production and injection are only possible when the rock develops permeability<sup>17</sup>. The rock permeability may be developed by:
  - a. the crushing of the diatomite near to the producers due to pore pressure depletion
  - b. the liquefaction of the diatomite near the injectors
  - c. the creation of "flow tubes" between injectors and producers
  - d. the reconnection of natural fractures and faults.
2. There are several spatial and temporal scales governing the hydrocarbon production and water injection into the Lost Hills diatomite. Areal, the Lost Hills field is partitioned into the flow compartments by a network of major faults. Vertically, as a result of the cyclic depositional environment<sup>18</sup>, the diatomite is layered across width scales ranging from tens of meters to sub-millimeter. The inter-layer boundaries are weakly connected and ready to part when the fluid pressure changes<sup>17</sup>.
3. The steady-state flow component of the injected water is considerable: much of the injected water flows through the "flow tubes" and/or along the faults and natural fractures. This type of flow is very fast compared with the spontaneous imbibition into the diatomite rock.
4. The injected water provides pressure support, but at a cost of significant recirculation.

### Nomenclature

$Y$  = effective fracture are, Bbl/psi/day<sup>1/2</sup>  
 $Z$  = absolute permeability of the reservoir, Bbl/psi/day  
 $P$  = injection reservoir pressure, psi  
 $Q$  = fluid flow rate, Bbl/day

### Acknowledgments

The authors would like to thank ChevronTexaco, Lawrence Berkeley National Laboratory and U.C. Oil® Consortium for their permission to publish this paper. The Assistant Secretary for Fossil Energy, Office of Gas and Petroleum Technology, provided partial support for this work under contract No. DE-ACO3-76FS00098 to the Lawrence Berkeley National Laboratory of the University of California. Partial support was provided by a member of the U.C. Oil® Consortium, ChevronTexaco. Portions of this work were performed at the Jet Propulsion Laboratory, California Institute of Technology under contract with the National Aeronautics and Space Administration.

This work could not have been done without the help of the Lost Hills Team members. The authors wish to recognize all the team members, both past and present.

### References

- Silin, D.B. and T.W. Patzek: "Control model of water injection into a layered formation," *SPE Journal*, (2001) **6** 253.
- Wallace, N.J. and E.D. Pugh: "An Improved Recovery and Subsidence Mitigation Plan for the Lost Hills Field, California," paper SPE 26626 presented at the 1993 SPE Annual Technical Conference and Exhibition Conference, Houston, Oct 3-6.
- Patzek, T.W., D.B. Silin, and E.J. Fielding: "Use of Satellite Radar Images in Surveillance and Control of a Two Giant Oilfields in California," paper SPE 71610 presented at the 2001 SPE Annual Technical Conference and Exhibition Conference, New Orleans, September 30-October 3.
- Cales, G.L., *et al.*: "Subsidence Remediation - Extending Well Life Through the use of Solid Expandable Casing Systems," paper presented at the 2001 American Association of Drilling Engineers Conference, Houston, March 27.
- Zhou, D., J. Kamath, and F. Friedmann: "Identifying Key Recovery Mechanisms in a Diatomite Waterflood," paper SPE 75142 presented at the 2002 SPE/DOE 3rd Symposium on IOR Conference, Tulsa, April 15-17.
- Wilt, M., *et al.*: "Using Crosswell Electromagnetics to Map Water Saturation and Formation Structure at Lost Hills," paper SPE 68802 presented at the 2001 SPE Western Regional Conference, Bakersfield, March 26-30.
- Emanule, M.A., *et al.*: "A Case History: Completion and Stimulation of Horizontal Wells with Multiple Transverse Hydraulic Fractures in the Lost Hills Diatomite," paper SPE 39941 presented at the 1998 SPE Rocky Mountain Regional Conference, Denver, April 6-8.
- Wright, C.A. and R.A. Conant: "Hydraulic Fracture Reorientation in Primary and Secondary Recovery from Low-Permeability Reservoirs," paper SPE 30484 presented at the 1995 SPE Annual Technical Conference & Exhibition Conference, Dallas, October 22-25.
- Wright, C.A., *et al.*: "Downhole Tiltmeter Fracture Mapping: A New Tool for Directly Measuring Hydraulic Fracture Dimensions," paper SPE 49193 presented at the 1998 SPE Annual Technical Conference and Exhibition Conference, New Orleans, Sept. 27-30.
- Silin, D.B. and T.W. Patzek: "Water injection into a low-permeability rock - 2: Control model," *Transport in Porous Media*, (2001) **43** 557.
- Patzek, T.W. and D.B. Silin: "Water Injection into a Low-Permeability Rock - 1. Hydrofracture Growth," *Transport in Porous Media*, (2001) **43** 537.
- Barenblatt, G.I., T.W. Patzek, V.M. Prostokishin, and S. D.B.: "New challenge for subterranean mechanics.," paper presented at the 2002 San Antonio.
- Bürgmann, R., P.A. Rosen, and E.J. Fielding: "Synthetic Aperture Radar Interferometry to Measure Earth's Surface Topography and its Deformation," *Ann. Rev. Earth Planet. Sci.*, (2000) **28** 169.
- Borgeaud, M. and U. Wegmüller: "On the Use of ERS SAR Interferometry for the Retrieval of Geo- and Bio-Physical Information," paper presented at the 1996 ERS SAR Interferometry Workshop 1996 Conference, Remote Sensing Laboratories, University of Zürich, 30 Sept - 2 Oct.
- Fielding, E.J., R.G. Blom, and R.M. Goldstein: "Rapid subsidence over oil fields measured by SAR interferometry," *Geophysical Research Letters*, (1998) **V25** 3215.
- Gesch, D., *et al.*: "The National Elevation Dataset," *Journal of the American Society for Photogrammetry and Remote Sensing*, (2002) **68** 5.
- Barenblatt, G.I., T.W. Patzek, V.M. Prostakishyn, and D.B. Silin: "Oil Deposits in Diatomites: A New Challenge for Subterranean Mechanics," paper SPE 75230 presented at the 2002 SPE/DOE 3th Symposium on IOR Conference, Tulsa, April 15-17.
- Schwartz, D.E., *Characterizing the Lithology, Petrophysical Properties, and Depositional Settings, South Belridge Field, Kern County, CA.*, in *Studies of the Geology of the San Joaquin Basin*, S.A. Graham, and Olson, H. C., Editor. 1988, The Pacific Section Society of Economic Paleontologists and Mineralogists: Los Angeles, CA.

### SI Metric Conversion Factors

acre	x 4.046 873	E+03 = m <sup>2</sup>
°API	141.5/(131.5+°API)	= g/cm <sup>3</sup>
bbl	x 1.589 873	E-01 = m <sup>3</sup>
cp	x 1.0*	E-03 = Pa s
ft	x 3.048*	E-01 = m
ft <sup>3</sup>	x 2.831 685	E-02 = m <sup>3</sup>
°F	(F-32)/1.8	= °C
in.	x 2.54*	E+00 = cm
md	x 9.869 233	E-04 = μm <sup>2</sup>
psi	x 6.894 757	E+00 = kPa

\*Conversion factor is exact.